Automated Parametric Optimization of a High-Purity Germanium Monte Carlo Neutral-Particle Model

Bryan V. Egner,* Robert S. Torzilli*

**Air Force Institute of Technology, 2950 Hobson Way, Wright-Patterson AFB, OH 45433, Bryan.Egner@afit.edu*

INTRODUCTION

Gamma-ray spectroscopy using high-purity germanium (HPGe) detectors is a leading method for obtaining high-energy-resolution spectra in both the field and laboratory settings. These detectors have the ability to obtain energy resolutions as low as 0.15 keV for the Full-Width-Half-Maximum, at incident photons around 5.9 keV [1]. The tradeoff for high-energy resolution is an overall lower detection efficiency compared to other types of detectors, such as sodium Iodide scintillators. The advancement of radiation transport codes, such as Monte Carlo Neutral-Particle (MCNP6), allows researchers to accurately model detection responses of HPGe detectors at various geometries, source energies, and environments [2].

Unfortunately, creating a MCNP detector model accurately representing reality can be difficult and time consuming, thus applying a systematic computational approach can streamline the process. Rather than manually carrying out trial-and-error adjustments to match experimental data, development of an automated parametric optimization code will simplify the enhancement of a rudimentary HPGe detector model.

Problem Description

Factors to consider when developing a MCNP detector model include the following: the type and position of the radiation source; the properties, both geometrical and compositional; and the characteristics of primary and secondary incident radiation. Published literature has stated relative differences between the experimental and Monte Carlo simulated full-energy peak absolute efficiencies for HPGe detectors have reached as low as 0.2% [3]. There have also been studies showing discrepancies between the detector specifications of internal components compared to measured values, such as the crystal length and dead layers [4].

Experimental measurements of gamma-ray emissions using a standard Canberra p-type HPGe detector were provided by Lieutenant Colonel (LTC) Buckley O'Day, at the Air Force Institute of Technology (AFIT), using a calibration multi-nuclide source manufactured by Eckert & Ziegler Isotope Products. The multi-nuclide source covered photon energies ranging from 59.9 to 1836 keV, allowing for a full representation of the absolute efficiency curve.

A labeled diagram of the various source positions with respect to the HPGe detector and base of the lead shield is shown in Figure 1. At each position, a 24-hour count was performed to minimize uncertainty. For position 1, the source was centered on the Al casing, position 2 was resting on the front face and flush with the edge of the casing, position 3 was centered 7 cm above the front face, position 4 was placed 3 cm down the side of the casing, and position 5 was offset 13 cm above the detector.

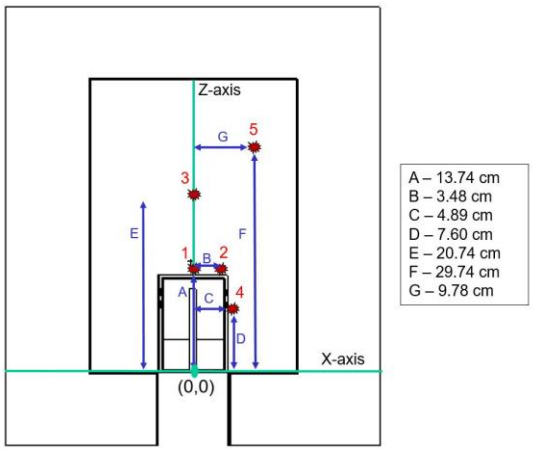

Fig. 1. Experimental setup diagram displaying each source position on a Cartesian coordinate system. The origin is centered at the base of the Al casing of the detector.

A plot of the spectra and the calculated absolute efficiencies as a function of energy were also provided by LTC O'Day for comparison with the simulated results. The absolute efficiency was calculated using Equation 1.

$$\varepsilon_{abs} = \frac{N_c}{\gamma * A_0 * t_l * \exp[-\frac{ln2}{t_h} * t_d]} \quad (1)$$

N_c is the total number of counts under the full-energy peak. A_0 is the initial activity of the source, multiplied by the live time, t_l, in seconds. The source decay is accounted for by multiplying the denominator by the decay exponential where t_h is the half-life and t_d is the age of the source, both in seconds.

DESCRIPTION OF WORK

First, a HPGe detector model was created using MCNP, and then an optimization code was produced in Python. After the model was optimized, efficiency curves were plotted for a quantitative analysis.

HPGe MCNP Model

The MCNP model was designed based off the manufacturer provided detector diagram labeled with

various dimensions and materials. Unfortunately, some dimensions were not labeled, including information about the internal contact pin, gap widths between the Ge crystal and the inner Al holder, and the insulation materials. For higher energy photons, these features are not as important, but for the lower energies, attenuation is more probable to occur which might affect the efficiency calculations. The goal of the generic MCNP model was to have easily adjustable parameters, thus only right circular cylinders and planes were utilized in the model geometry. The only changes needed to be made would be raising or lowering the heights, and widening or compressing the widths to adjust detector parameters. The final design of the generic HPGe MCNP model outputted in VisEd and illustrated in Figure 2.

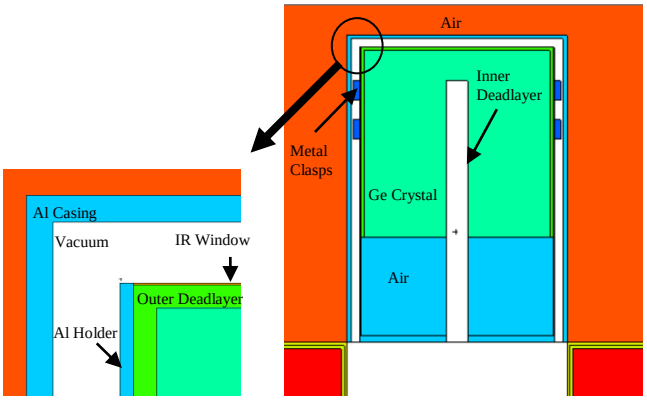

Fig. 2. Generic HPGe Model displayed using VisEd. An enlarged view of the top edge of the Ge crystal is shown.

The infrared window placed directly above the top deadlayer is composed of a thin 1E-02 cm kapton tape window and an 8.47E-04 cm Al Mylar layer. Both the HPGe crystal top edges and the top of the inner coaxial were assumed to be squared, rather than rounded, since the manufacturer did not specify these features. In the left image of Figure 2, the outer deadlayer can be seen and was assumed to be a lithium drifted surface. The inner deadlayer was assumed to be a boron implanted contact. Neither of these materials were explicitly stated in the detector schematic, and the compositional assumptions were based on common p-type HPGe detector fabrication techniques [1]. All material composition data were found in resources published by Los Alamos and Pacific Northwestern National Laboratories [5, 6]. The cross-sectional data library used was mcplib84 (.84p) for photon transport utilizing 278 energy groups.

Since only the absolute efficiency was desired, producing a full-energy spectrum is unnecessary and Gaussian energy broadening was neglected. The default Physics Card settings were used, meaning Bremsstrahlung, coherent scattering, and photo-fission were ignored as well. The source card represented the multi-nuclide source as an isotropic point source emitting 12 discrete photon energies, each with the same probability distribution to avoid large statistical variations in each source from differing emission rates. The energy deposition, F8, tally was used to track particle interactions with the Ge crystal, and 10^6 source particles were used to reduce uncertainties.

After the model was created, a review of previous research led to the conclusion that the deadlayers, entrance windows, HPGe crystal length, and radius had the largest effect on modeling HPGe detection efficiency [3, 4]. A full list of model parameters adjusted and the order of adjustments can be found in Table I of the results section.

Automated Parametric Optimization Code

The MCNP Automated Parameters, MAP, Python code developed uses user supplied data, points, parameters of interest and their associated range, and a prepared MCNP input deck to create an experimentally observed detector. It accomplishes this task by iterating through all defined points for each parameter while keeping the values that minimize the chi-squared value

$$X^2 = \sum_{i=0}^{N} \frac{(D_a - D_e)^2}{\sigma^2} \quad (2)$$

where D_a is the analytical derived efficiency created by MAP, D_e is the experimental efficiency that MAP is trying to match, and σ is the uncertainty of the experimental data. The closer chi squared is to one, the better fit the model is to the experimental data. The process that MAP currently uses to determine which values are the best is a brute force method. By comparing the previous best chi squared value with the current one for every step in the user supplied range it can make a reasonable decision on what would be the best value to use for each parameter. Once it has determined the optimum result it can achieve from that parameter's given range, it moves on to the next parameter and repeats this process.

MAP's secondary purpose is to automate the collection of relevant data for the purpose of recording what other parameters could be of interest based on how it affects the overall data. This is accomplished by printing out the relative difference between the experimental and MCNP absolute efficiencies, the average relative difference, and plots of the data superimposed upon the experimental data in an easy to read format. From these outputs, the user can determine if an interested parameter is behaving as expected or if it even affects the model in a meaningful way. This makes it easier to determine what values need to be adjusted as well as what could be occurring to cause a difference in the model versus the experiment.

RESULTS

Five efficiency curves were produced from the output of the F8 tallies, and the results are shown in Figures 3 through 7. In the experimental data, a systematic jump in

efficiency at 320 keV for positions 1, 2, 3, and 4 was evident and so the Cr-51, 320 keV photopeak efficiency was neglected and Sr-85 was neglected from position 5 because the jump shifted to 514 keV. Thus the number of degrees of freedom, ν, was equal to 10 because 11 photon energies were used for the efficiency curves. Figure 3 displays the experimental and MCNP absolute efficiencies for source position 1 where the average relative difference was 52%, and the minimum relative difference was 2%. The experimental and MCNP results match up fairly well for energies above 159 keV being less than 10%, but the lower energies have 100% or more, relative difference.

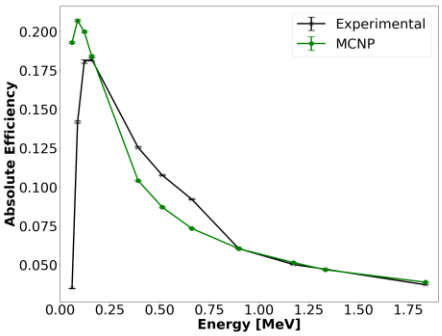

Fig. 3. Experimental and MCNP absolute efficiency as a function of photon energy at position 1.

The results for position 2 and 3, displayed in Figure 4 and Figure 5 respectively, showed a similar behavior as position 1; where the experimental efficiencies for lower energy photons varied drastically compared to the MCNP model.

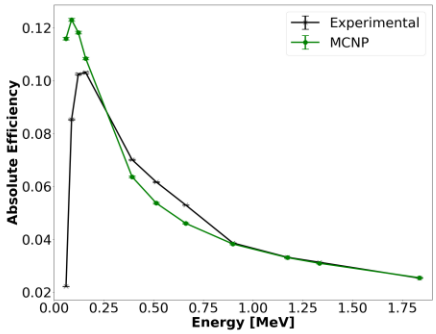

Fig. 4. Experimental and MCNP absolute efficiency as a function of photon energy at position 2.

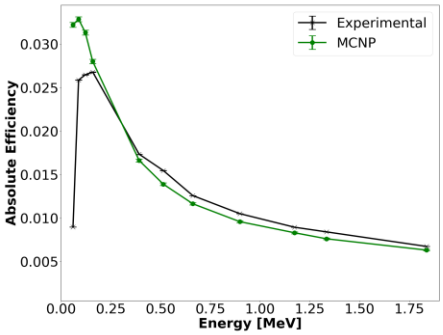

Fig. 5. Experimental and MCNP absolute efficiency as a function of photon energy at position 3.

When the source was placed on the side of the HPGe detector, the experimental and MCNP efficiencies were not in agreement, as shown in Figure 6. This may have occurred from incorrectly modeling the experimental setup, for a source placed near the side of the Al casing.

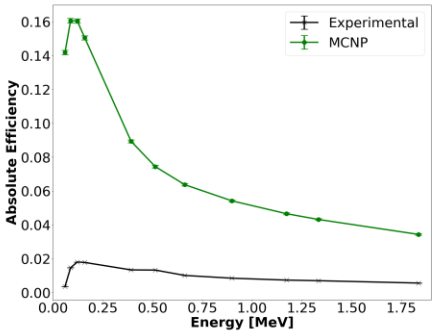

Fig. 6. Experimental and MCNP absolute efficiency as a function of photon energy at position 4.

The results for the final position for a source offset and 13 cm above the detector had a similar efficiency curve shape to positions 1, 2, and 3, as shown in Figure 7.

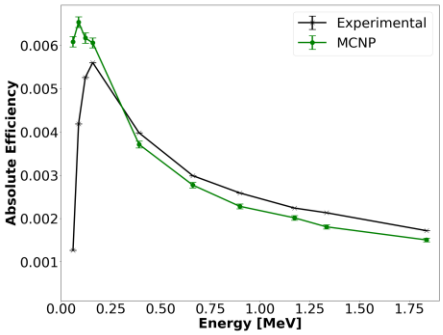

Fig. 7. Experimental and MCNP absolute efficiency as a function of photon energy at position 5.

The final parameters outputted by the automated optimization code are shown in Table 4. Most of the adjustments for each source position were similar, where the top deadlayer increased and the crystal length shortened to account for pileup, electric field, and other losses not captured in the MCNP model by pure photon transport.

TABLE I. Optimized Detector Parameters

Parameter	Initial Value	Position: 1	2	3	4	5
Outer Top Deadlayer [cm]	0.13	0.739	0.739	0.739	0.739	0.739
Outer Sides Deadlayer [cm]	0.13	0.23	0.23	0.23	1.35	0.23
Ge Crystal Length [cm]	8.32	7.66	7.48	7.48	7.48	7.48
Kapton Window [cm]	0.010	0.110	0.110	0.110	0.058	0.110
Inner Top Coaxial Deadlayer [cm]	3E-05	1E-04	6E-05	6E-05	1E-04	6E-05
Inner Sides Coaxial Deadlayer [cm]	3E-05	2E-05	6E-05	7E-05	1E-3	7E-05
Top Al Casing Thickness [cm]	0.15	0.25	0.25	0.25	0.05	0.25
Sides Al Casing Thickness [cm]	0.15	0.05	0.05	0.05	0.27	0.25
Ge Crystal Density [g/cm^3]	5.32	5.32	5.32	5.32	5.32	5.32

The efficiency curves matched well at higher energies but poorly at energies below 159 keV. Another optimization trial was performed for positions 1, 2, 3, and 5 using only photon energies above 159 keV to observe the model performance, final relative differences and chi-squared values. The results can be seen in Table 5 and Figure 8. There was a stronger agreement between experimental and MCNP efficiencies with an average relative difference of 6.33%.

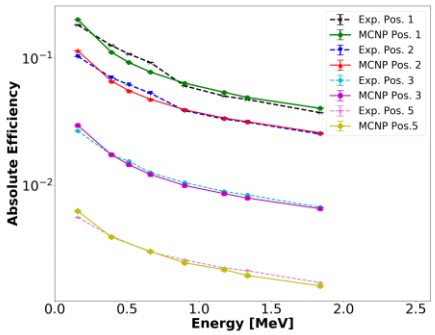

Fig. 8. Experimental and MCNP absolute efficiency as a function of photon energy at positions 1, 2, 3, and 5 for energies 159 keV and higher.

TABLE II. MCNP Model Performance, 159 – 1863 keV

Position	Average Relative Difference [%]	X^2/ν
1	9.44	8.67
2	5.51	3.83
3	4.66	2.36
5	5.73	2.91

CONCLUSION

The brute-force automated parametric optimization method produced a HPGe MCNP model that represents the absolute efficiency between energies of 159 to 1836 keV, with a relative difference less than 10% that improves as the source-to-detector distance is increased. Areas where the method failed to resemble experimentally obtained efficiencies are at low photon energies and locations where there would be more internal components holding the Ge crystal in place, such as source positions 2 and 4. These non-homogeneous regions of the HPGe detector near edges and deadlayers, where charge collection from the electric field in reality is imperfect are more difficult to match using MCNP. This is the case because this model designated the entire Ge crystal as a homogenous cell with ideal charge collection.

In the future, more adjustable parameters will be added to the optimization code along with more realistic radiation transport physics to reproduce experimental spectra. Efforts can be made to generalize the structure of the automation optimization code to be applicable for other detectors and experiments, as well as alternate means of optimization.

ACKNOWLEDGMENT S

We are grateful for the support of LTC O'Day and Capt James Bevins (AFIT) on completing this project.

DISCLAIMER

The views expressed in this article are those of the authors and do not reflect the official policy or position of the United States Air Force, Department of Defense, or the U.S. Government.

REFERENCES

1. G. F. KNOLL, *Radiation Detection and Measurement*, Hoboken, NJ: John Wiley & Sons, Inc., (2010).
2. D. B. Pelowitz, "MCNP6 User's Manual Version 1.0," Los Alamos National Laboratory, Los Alamos National Laboratory, 2013.
3. R. G. HELMER, R. G. HARDY, V. E. IACOB, M. SANCHEZ-VEGA, R. G. NEILSON and J. NELSON, "The use of Monte Carlo Calculations in the Determination of a Ge Detector Efficiency Curve," *Nuclear Instruments and Methods in Physics Research*, vol. 551, no. A, pp. 360-381 (2002).
4. R. M. KEYSER, "Resolution and Sensitivity as a Function of Energy and incident Geometry for Germanium Detectors," *Nuclear Instruments and Methods in Physics Research* Section B: Beam Interactions with Materials and Atoms, vol. 213, pp. 236-240 (2004).
5. L. CONLIN, "Listing of Available ACE Data Tables," Los Alamos National Laboratory, Los Alamos National Laboratory (2013).
6. R. MCCONN, "Compendium of Material Composition Data for Radiation Transport Modeling," Pacific North Western National Laboratory, Richland, WA (2011).
7. S. GUILHERME and J. D. S. CORRÊA, "Computational Modeling of a High Purity," in International Nuclear Atlantic Conference, Belo Horizonte, MG, Brazil, 2011.